Engineering Journal issn: 0125-8281

Article

Effects of Concrete Mix Proportion and Chloride Content on Electrochemical Properties of Reinforcing Steel in Concrete

Dong Viet Phuong Tran[1,a], Pakawat Sancharoen[2,b,*], Pitichon Klomjit[3], and Somnuk Tangtermsirikul[1]

1 School of Civil Engineering and Technology, Sirindhorn International Institute of Technology (SIIT), Thammasat University, Thailand
2 Construction and Maintenance Technology Research Center (CONTEC), School of Civil Engineering and Technology, Sirindhorn International Institute of Technology, Thammasat University, Thailand
3 National Metal and Materials Technology Center (MTEC), Thailand
E-mail: [a]tvpdong@gmail.com, [b]pakawat@siit.tu.ac.th (Corresponding author)

Abstract. Corrosion of steel in concrete has been considered as a major cause reducing the lifespan of reinforced concrete (RC) structures. Evaluation of corrosion rate is crucial to determine service life and maintenance plaining for RC structures. Electrochemical properties of corrosion of embedded steel in concrete, including the Tafel slope, corrosion potential and corrosion current density, are significant parameters predicting corrosion rate. The objective of this paper was to quantitatively evaluate electrochemical properties of steel in different compositions of concrete. Varied parameters include the water to binder ratio of concrete, type of binder and chloride content. The electrochemical properties were evaluated at three periods of exposure. Experimental results reveal that the electrochemical properties of reinforcing steel depend on water to binder ratio, type of binder and chloride content. An increase in chloride content significantly decreases the corrosion potential and increases the corrosion rate of steel. The anodic equilibrium potential is lower with an increase in chloride content. The varied concrete mix proportion significantly influence the cathodic polarization. This is due to the effects of concrete porosity on oxygen concentration, which is influenced by the concrete mix proportions. The results can be used to predict corrosion rate of steel in various concrete mix proportion for determining service life and repairing of RC structures.

Keywords: Rebar corrosion, reinforced concrete, electrochemical properties.

ENGINEERING JOURNAL Volume 24 Issue 3
Received 19 August 2019
Accepted 27 February 2020
Published 31 May 2020
Online at https://engj.org/
DOI:10.4186/ej.2020.24.3.23

DOI:10.4186/ej.2020.24.3.23

1. Introduction

For many years, reinforcement corrosion has been considered as the major problem reducing the lifespan of reinforced concrete (RC) structures. Particularly, those RC structures locating in marine environment, have been significantly deteriorated by chloride attack. Along with the unexpected increase in chloride content, the variation of concrete compositions, such as water to binder ratio, fly ash content, etc., could affect the state of reinforcement corrosion. The severity of corrosion is normally evaluated based on electrochemical properties such as electrical resistivity of concrete, corrosion potential and corrosion rate of reinforcing steel [1-9]. Moreover, the other electrochemical properties such as Tafel slope and equilibrium potential, can be used to simulate both anodic and cathodic polarization in corrosion process. Understanding the anodic and cathodic polarization, repairing of the corroding RC structures can be well designed and conducted.

Tafel slope is widely used to calculate corrosion rate of steel based on Stern-Geary equation [10-12]. Previously, the variation of Tafel slope and equilibrium potential were observed during the process of corrosion. Hussain et al. [13] showed that an increase in chloride content may reduce the anodic Tafel slope and anodic equilibrium potential, which then led to the increase of corrosion rate of reinforcing steel. Without the presence of chloride ion in concrete, the potential on the surface of reinforcing steel was stable in a wide range of potential. The increase in chloride content shortened the stable potential range on surface of steel. Hence, reinforcing steel change easily from the passivity stage to the pitting stage, where the change of potential contributes to a remarkable increase in corrosion current density. Besides, the availability of oxygen in concrete affected the cathodic polarization curve. The magnitude of cathodic Tafel slope increased when the concentration of oxygen decreased. In accordance with this, corrosion potential became more negative but lower corrosion rate of steel was found to be lower [14].

In this study, concrete mix proportion and chloride content were varied aiming to investigate the variation of electrochemical properties of reinforcing steel in various concrete. The concerning properties of steel included Tafel slope, equilibrium potential, corrosion potential and corrosion rate. Potentiodynamic measurement was conducted to determine the electrochemical properties of reinforcing steel.

2. Experimental Program

2.1. Materials

In this study, the materials used to mix concrete were: Ordinary Portland cement (OPC) - cement type I according to ASTM C150 [15], crushed lime-stone and river sand with their specifications following the requirements of ASTM C33 [16], coal fly ash (FA) type 2b according to TIS2135 [17] and tap water. The parameters were varied as shown below:

– Water to binder ratio: 0.45 and 0.6;
– Percentage of fly ash: 0 and 30% by weight of binder;
– Chloride content: 0, 1%, and 2% by weight of concrete.

Table 1 shows the concrete mix proportions that were used to cast the specimens. To simulate an aggressive environment, a specific amount of sodium chloride (NaCl) was pre-mixed in the mixing water of concrete to obtain chloride content as previously mentioned. One steel bar, DB20 grade SD40 with a diameter of 20 mm and a length of 200 mm, was embedded in each specimen. Figure 1 illustrates the preparation of steel bar with an epoxy coating at both ends of the steel bar and the remaining exposed surface area of the steel bar was kept constant at 50 cm^2.

2.2. Specimen Preparation

Reinforced concrete (RC) specimens used in this study were cubic, 100x100x100 mm with 200mm-long DB20 steel bar extruding from one side. Figure 2(a) shows a picture of the RC specimen. The covering depth was fixed at 20 mm.

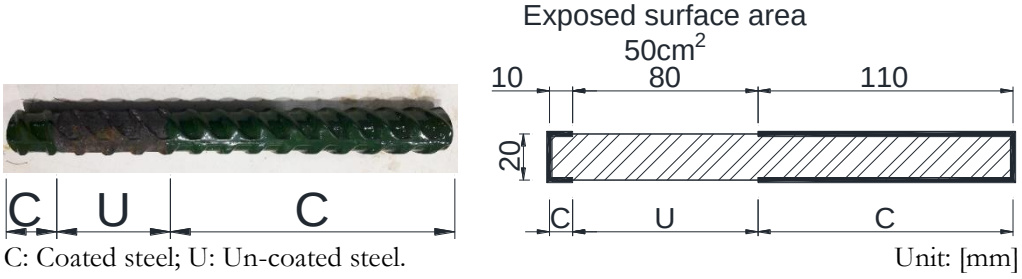

Fig. 1. Preparation of steel bars embedded in the concrete specimen.

Table 1. Concrete mix proportions.

No.	W/B ratio	Fly ash (%)	Unit content (kg/m³)				
			Cement	Fly ash	Fine aggregate	Coarse aggregate	Water
1	0.45	0	421	0	743	1045	190
2	0.45	30	280	120	743	1045	180
3	0.6	0	352	0	743	1045	211
4	0.6	30	236	101	743	1045	202

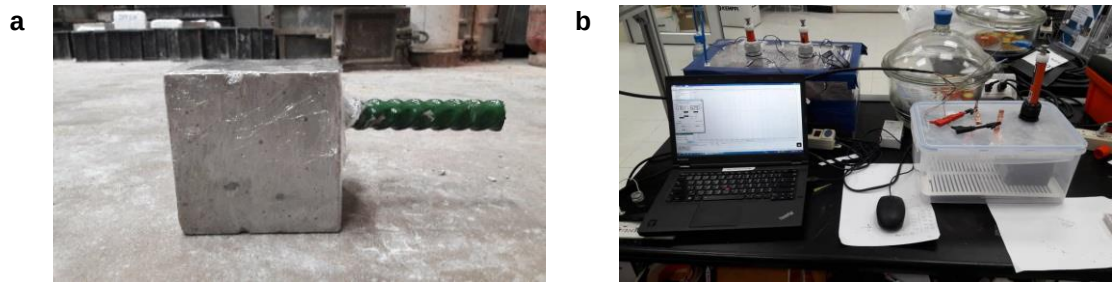

Fig. 2. (a) Reinforced concrete specimen; (b) Set up for potentiodynamic measurement.

2.3. Potentiodynamic Measurement

To determine the electrochemical properties of reinforcing steel, a potentiodynamic measurement was conducted with the set-up as shown in Fig. 2(b). The components of the measurement system include four main parts: the potentiostat (Autolab PGSTAT302N), reference electrode ($Cu/CuSO_4$), counter electrode (stainless steel grade 304) and working electrode (reinforcing steel). To ensure good connectivity among the components, conductive copper tape was used as a connector and conductive gel was used between the stainless steel and the concrete surface. The measurement parameters are provided as follows:

- Time for determining open-circuit potential (OCP): 300 s;
- Potential sweep range: ±120 mV around OCP;
- Potential sweep rate: 0.5 mV/s.

During the measurement, the ambient environment surrounding the specimens was controlled by placing the specimens in a closed plastic box. This minimized the loss of moisture in concrete cover, which may significantly influence the polarization behavior.

Figure 3(a) shows the raw data obtained from the measurement. The collected data from the measurement can be analyzed to extract the polarization behavior of reinforcing steel, as described in Fig. 3(b). Based on a suggestion of previous studies [18, 19], a developed fitting algorithm was used to extract the electrochemical properties of reinforcing steel from the collected data of measurement. The corrosion rate was calculated from the corrosion current by applying Faraday's equation, as described in Eq. (1) [20].

$$CR = \frac{EW \times T \times I}{A \times F} \times 1000 \quad (1)$$

where: CR (mg/cm².year) is the theoretical mass loss of reinforcing steel, EW (≈28 g/mol) is the equivalent weight of the carbon steel, T (s) is the exposure period, I (A) is the corrosion current; A (cm²) is the exposed surface area, and F (≈96,500 C/mol) is Faraday's constant.

The slopes of fitted linear lines represent the anodic and cathodic Tafel slopes. Finally, the equilibrium potential could be linearly extrapolated based on the exchange current density. The exchange current density depends on the intrinsic nature of each metal, and also depends on the surface characteristics of the specific metal [21]. In this study, since only one type of steel was used, the exchange current densities were fixed for anodic and cathodic polarization, $i_{0a} = 10^{-5}$ A/m² and $i_{0c} = 10^{-10}$ A/m² [18].

DOI:10.4186/ej.2020.24.3.23

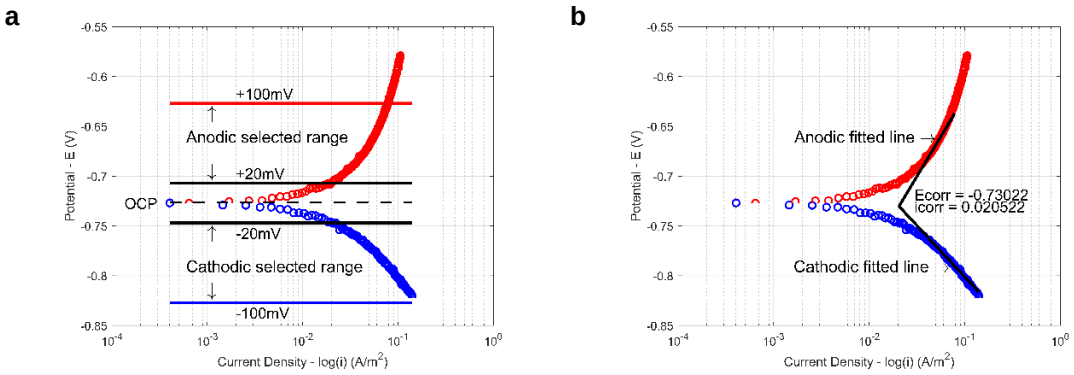

Fig. 3. Example of collected and analyzed data of potentiodynamic measurement: (a) Raw data with selected range for fitting; (b) Fitted lines after analyzing raw data.

3. Results and Discussion

3.1. Corrosion Potential and Corrosion Rate

3.1.1. Corrosion potential

As can be seen in Fig. 4, the corrosion potential (V. vs CSE) is lower when the chloride content in the concrete increases. Moreover, the corrosion potential is found to be lower with an increase in the exposure period. According to ASTM C876 [22], the more negative the steel potential, the higher the possibility of the corrosion of reinforcing steel, as described in Table 2.

At 2 months, the corrosion potential of reinforcing steel in free chloride specimens is about -200 mV, which results in the 10% possibility of corrosion based on ASTM C876 [22]. Compared to the chloride-contaminated concrete, the corrosion potential is approximately -550 mV, which means that reinforcing steel has a high possibility to corrode. The appearance of chloride in concrete destroys the passive film on the surface of reinforcing steel or even prevents the formation of a passive film. Without protection from the passive film, the potential on the surface of reinforcing steel was not stable. At a longer period, a similar pattern can be observed. At 6 months, the corrosion potential of chloride-free ordinary Portland cement (OPC) concrete with 0.6 W/B is -620 mV, which is higher than that of OPC concrete with 1% [Cl-] (-680 mV) (Fig. 4(b)). At a later age, the corrosion potential of chloride-free concrete exhibited a very low value, because of the exposure conditions used in this study (high humidity). The potential of reinforcing steel can exhibit very low when RC specimen is kept in these conditions for a long time. Similar results with a very negative potential of steel were found by previous researchers [23-26].

The effects of the concrete parameters on corrosion potential were observed after a long term exposure period. It is worth mentioning that the variation of corrosion potential due to the influence of concrete parameters was lower than that due to chloride content. After 2 months, reinforcing steel in chloride-free concrete with 0.45 W/B had a higher potential than that with 0.6 W/B. For example, the corrosion potential of OPC concrete with 0.45 W/B is -180 mV (Fig. 4(a)), while that with 0.6 W/B is -220 mV (Fig. 4(b)). The reason for this phenomenon is that the porosity of 0.45 W/B concrete is lower than that of 0.6 W/B concrete. Low porosity concrete constrained the penetration of corrosive factors such as water, oxygen, etc. Even in chloride-contaminated concrete, the aforementioned phenomenon can be observed. There was a higher amount of cement used in low W/B concrete, which slightly increased the pH level. As a result, passive films on the surface of reinforcing steel were stronger.

Regarding the effects of fly ash on corrosion potential, there are three aspects that should be considered: First, a decrease in the porosity of concrete; second, a reduction of free chloride in chloride-contaminated concrete; and third, decrease in pH. For the first aspect, the pozzolanic reaction in fly ash concrete decreases the porosity of concrete, which contributes to a more positive corrosion potential. From the experimental results, this could not be observed in chloride-free concrete at this time because the pozzolanic reaction takes more time to develop. Second, the introduction of fly ash reduces the content of free chloride, which is the main factor inducing the corrosion of reinforcing steel. Fly ash can minimize free chloride ions due to better chloride binding capacity [27, 28]. This phenomenon could be observed in the experimental results. Third, according to previous findings, the pH of OPC concrete is higher (more alkaline) than that of FA concrete [29, 30]. Due to this drop in pH in FA concrete, passive films on the surface of steel could be weakened. In theory, the interaction of reinforcing steel with the highly alkaline environment (pH = 12 to 13 [24]) of concrete leads to the formation of a protective film on the steel surface. A pH lower than 10.5 causes passive film instability and thus a lower corrosion potential. However, the effects of this aspect on the corrosion potential could not be found in our experimental results, even in chloride-free and chloride-contaminated concrete. The reason is that although fly ash tends to decrease the pH of the concrete, the decrease is very small, as the surrounding environment is still sufficiently alkaline. The effects of pH can be considerable on other electrochemical properties, which is discussed below.

The corrosion potential decreased significantly when the exposure time is increased in both chloride-free and

chloride-contaminated concrete. This is caused by corrosive agents, such as water and oxygen, continuously accumulated on the steel surface, which results in the progression of corrosion of reinforcing steel. The corrosion potential becomes lower with time. In other words, the possibility of corrosion of steel increased with time.

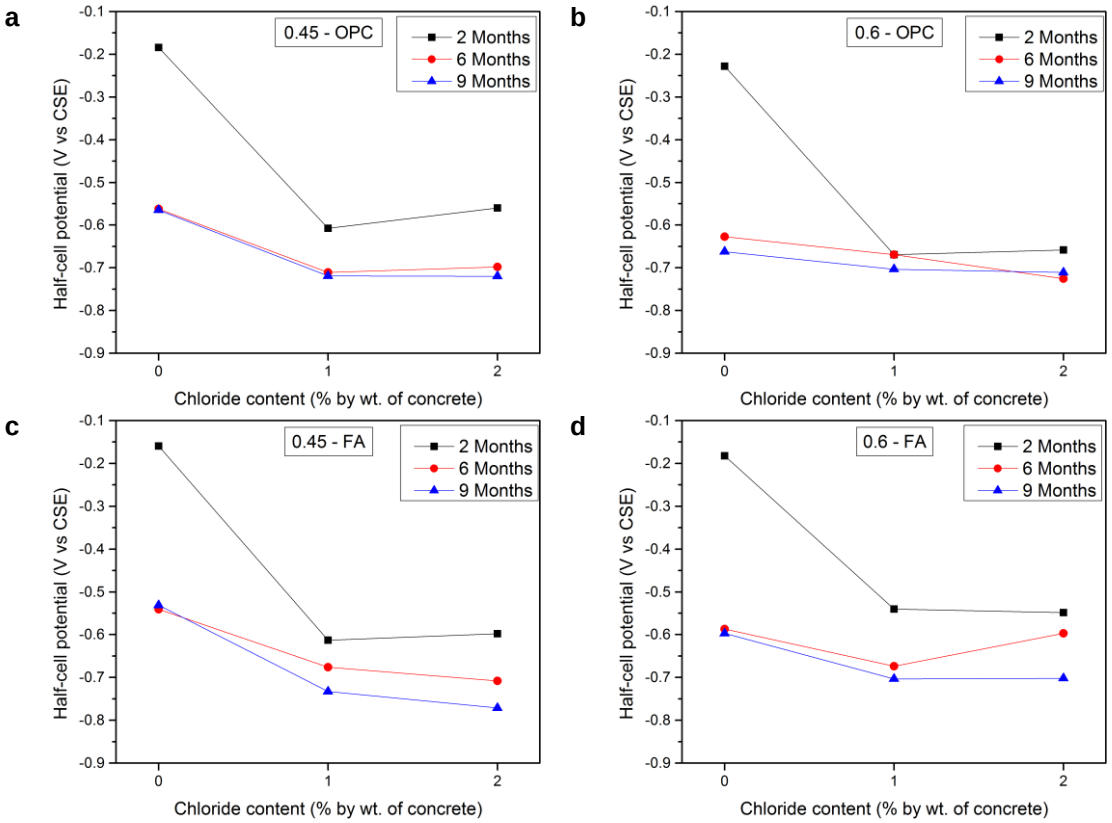

Fig. 4. Corrosion potential in (a-b) OPC concrete with W/B ratio (a) 0.45 and (b) 0.6 and (c-d) FA concrete with W/B ratio (c) 0.45 and (d) 0.6.

Table 2. Relationship between corrosion potential and possibility of corrosion.

Corrosion potential (mV. CSE)	**Possibility of corrosion**
> -200	Low (less than 10%)
-200 – -350	Intermediate corrosion risk
< -350	High (more than 90%)
<-500	Severe corrosion

3.1.2. Corrosion rate

Figure 5 illustrates the corrosion rate (mg/cm^2·year) of reinforcing steel in concrete with different parameters, including chloride content, water to binder ratio, content of fly ash, and exposure period. With 2 months of exposure, the chloride ions increased the corrosion rate of reinforcing steel in concrete. The chloride in concrete accelerated the dissolution reaction of steel. An increase in chloride ions adds electrolytes in the concrete pore solution, leading to a decrease in concrete resistivity [14]. Solid salts, specifically NaCl, can absorb water to form aqueous electrolytes, which then offers good conductivity for corrosion to occur [31]. This increase in moisture content makes the charged ions flow easily. Hence, the electrical resistivity of concrete decreases in chloride-contaminated concrete. The decrease in electrical resistivity encourages the transport of electrons between the anode and cathode, therefore the corrosion rate increases significantly.

DOI:10.4186/ej.2020.24.3.23

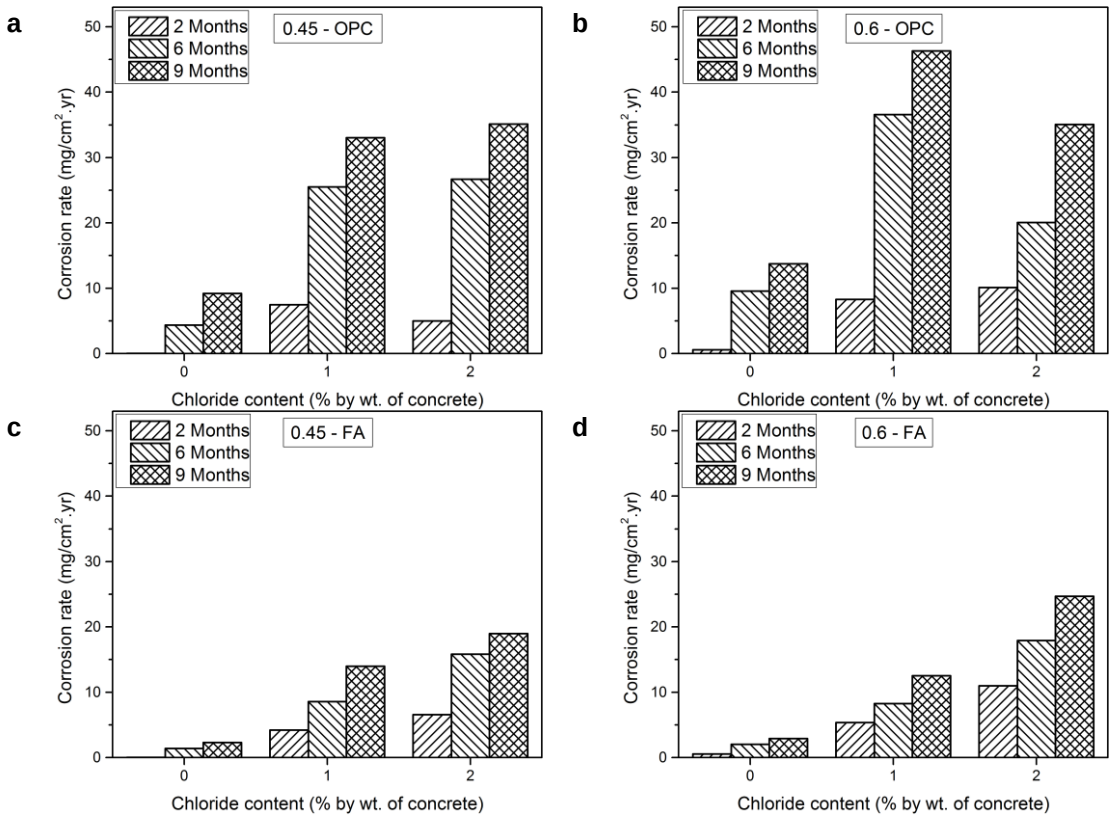

Fig. 5. Corrosion rate in (a-b) OPC concrete with W/B ratio (a) 0.45 and (b) 0.6 and (c-d) FA concrete with W/B ratio (c) 0.45 and (d) 0.6.

The concrete parameters play a crucial role in the change of corrosion potential and corrosion rate. Parameters of concrete were evaluated in two aspects: water to binder ratio and fly ash content. An increase in the water to binder ratio boosted the corrosion rate of reinforcing steel, which resulted from higher porosity of concrete. This higher porosity then eases the penetration of water and oxygen through the concrete cover. The corrosion rate of OPC concrete with 0.45 W/B and 2% [Cl^-] is 5.01 mg/cm²·yr (Fig. 5(a)) compared to that with 0.6 W/B which is 10 mg/cm²·yr after 2 months of exposure (Fig. 5(b)). Moreover, the lower electrical resistivity in high W/B concrete contributed to an acceleration of corrosion on the surface of reinforcing steel.

Additionally, fly ash (FA) can reduce the porosity of concrete, decreasing the free chloride content, and lowering pH of the concrete. After a certain period, the pozzolanic reaction of fly ash can reduce the porosity of the concrete. Therefore, the amount of oxygen and water are limited in the concrete and a higher electrical resistivity can be obtained in FA concrete compared to that in OPC concrete [7], especially at a later age. The penetration of oxygen through low porosity concrete is limited, resulting in the effects of concentration polarization on the corrosion process. Concentration polarization represents the effects of mass transport in an electrochemical process. In this case, it is the transportation of oxygen. As a result, the corrosion rate of reinforcing steel in FA concrete is lower than that in OPC concrete. In other aspects, chloride ions in concrete is captured by pozzolanic products to form bound chlorides. Regarding to chloride-induced corrosion, bound chlorides have no effects on the progress of reinforcement corrosion [14, 24]. The influence of the two mentioned factors decreased the corrosion rate of reinforcing steel in FA concrete. As can be seen in Fig. 5(d), the corrosion rate of FA concrete with 0.6 W/B and 1% [Cl^-] is 5.20 mg/cm²·yr compared to that of OPC concrete which is 8.40 mg/cm²·yr after 2 months of exposure (Fig. 5(b)). For the influence of pH, the corrosion rate of reinforcing steel was higher in FA concrete than that in OPC concrete at the beginning of exposure. After 2 months of exposure, the corrosion rate of chloride-free OPC concrete with 0.6 W/B is 0.57 mg/cm²·yr, which is lower than that of FA concrete, 0.70 mg/cm²·yr. This is from the effect of a drop in pH surrounding the reinforcing steel, so that the dissolution of steel increased at an early stage. At a longer term, the FA concrete became denser, constraining the movement of corrosion current. For this reason, a low corrosion rate in FA concrete could only be found at a longer exposure period.

Within the period of this study, the corrosion rate of reinforcing steel increased gradually with time. The corrosion rate of reinforcing steel after 9 months of exposure was the highest. This phenomenon shows good agreement with the findings of previous researchers [8, 9]. The effects of the aforementioned factors, including water to binder ratio, fly ash and chloride content, still could be seen with increasing exposure period. The corrosion rate

in chloride-contaminated concrete was higher than that in chloride-free concrete. Lowering the water to binder ratio and replacing the cement with fly ash showed good results for minimizing the corrosion rate of reinforcing steel. Eventually, this increase in corrosion rate of reinforcing steel is related to the more negative corrosion potential with time.

3.2. Tafel Slope – β

3.2.1. Anodic Tafel slope

Figure 6 illustrates the anodic Tafel slope (β_a) of all specimens. The effects of chloride ions, water to binder ratio, fly ash content, and time of exposure were evaluated. Similar tendencies are observed at all periods of exposure. The anodic Tafel slope increased when the chloride ion concentration increased from 0 to 1%, followed by a decrease when increasing the concentration of chloride ions from 1% to 2%. In our experimental results, the correlation between the chloride content and the anodic Tafel slope cannot be observed at a very high chloride ions concentration. The anodic Tafel slope represents the degree of polarization at the anode (activation polarization). Activation polarization represents the charge transfer kinetics in the electrochemical process. The existence of chloride ions accelerates the dissolution of steel. As a consequence, the anodic Tafel slope is expected to decrease when more chloride is added in concrete, which was found by Hussain and Ishida [13]. It should be noted that the content of chloride used in this experiment is 6 times higher compared to that in previous research. The content of chloride was 0 to 10% by mass of binder in the work of Hussain and Ishida [13].

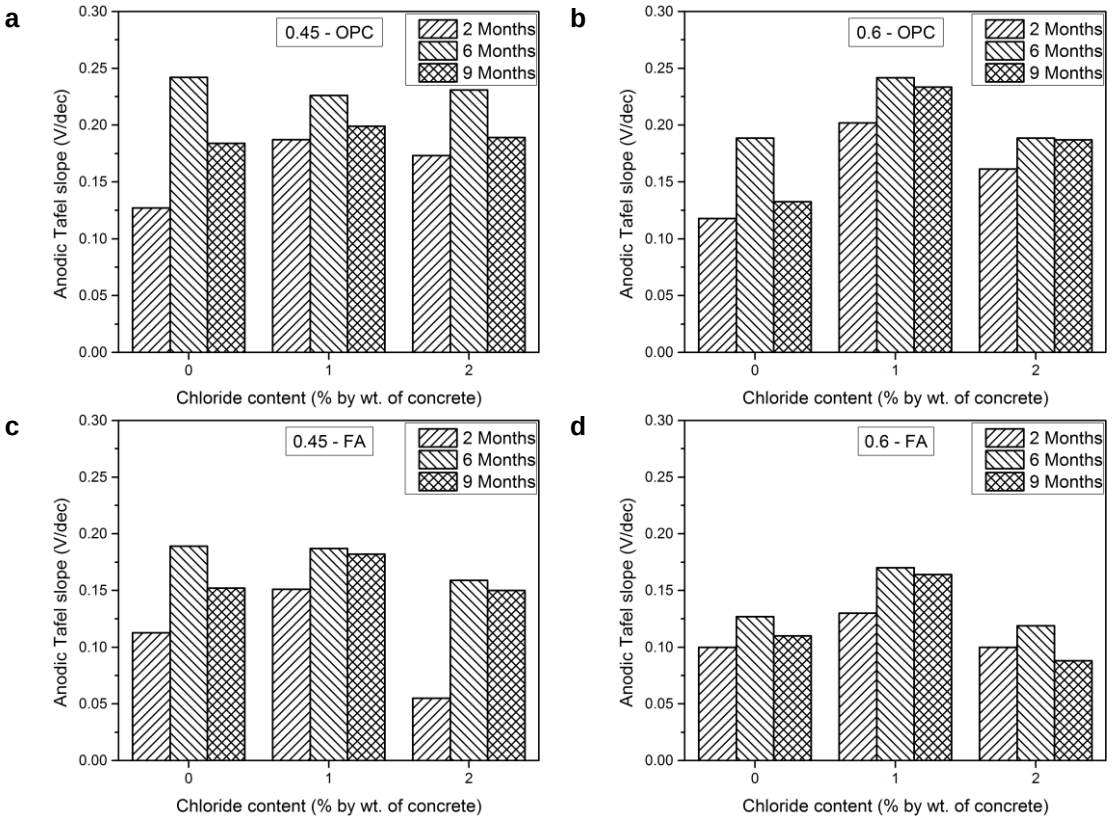

Fig. 6. Anodic Tafel slope in (a-b) OPC concrete with W/B ratio (a) 0.45 and (b) 0.6 and (c-d) FA concrete with W/B ratio (c) 0.45 and (d) 0.6.

Among all series, the parameters of concrete affected significantly the magnitude of the anodic Tafel slope. The water to binder ratio was inversely proportional to the anodic Tafel slope, which was the result of an increase in the porosity of concrete and a drop in pH. For the conditions of this study, high porosity concrete promotes high conductivity in the vicinity of reinforcing steel. Because of this phenomenon, reinforcing steel in concrete with 0.6 W/B has a lower anodic Tafel slope than that with 0.45 W/B. Subsequently, the inclusion of fly ash reduces the anodic Tafel slope, which was attributed to the decrease in pH. Although fly ash decreased the porosity of concrete and free chloride content, it also replaced a certain amount of cement which can lead to a drop in pH. The anodic Tafel slope in OPC concrete is higher than that in FA concrete, this phenomenon could be due the drop of pH in FA concrete. Variations of the anodic Tafel slope due to pH was also claimed by Ge and Isgor [32]. The corrosion rate in FA concrete is still low despite this decrease in anodic Tafel slope because of the effects of the low porosity of concrete and high electrical resistivity.

At all periods of exposure, the above mentioned patterns could be observed. However, the effects of long term exposure on the anodic Tafel slope cannot be

obtained according to our experimental results. Concrete is a heterogeneous material with the existence of pore structures and different moisture contents with time of exposure.

3.2.2. Cathodic Tafel slope

Figure 7 illustrates the experimental results of the cathodic Tafel slope (β_c) with various chloride contents, water to binder ratios, fly ash percentages, and time of exposure. The cathodic Tafel slope represents the degree of polarization at the cathode, including activation and concentration polarization. Besides the charge transfer, the mass transfer limitation also affects the electrochemical process, and is represented by concentration controlled polarization. The limitation of oxygen concentration increases the cathodic Tafel slope. Without chloride in concrete, oxygen diffuses into concrete more easily than through chloride contaminated concrete. For chloride-contaminated concrete, a high chloride ion concentration can encourage the concrete to retain water, which can limit the amount of oxygen. Consequently, the cathodic Tafel slope in chloride-free concrete is lower than that in chloride-contaminated concrete.

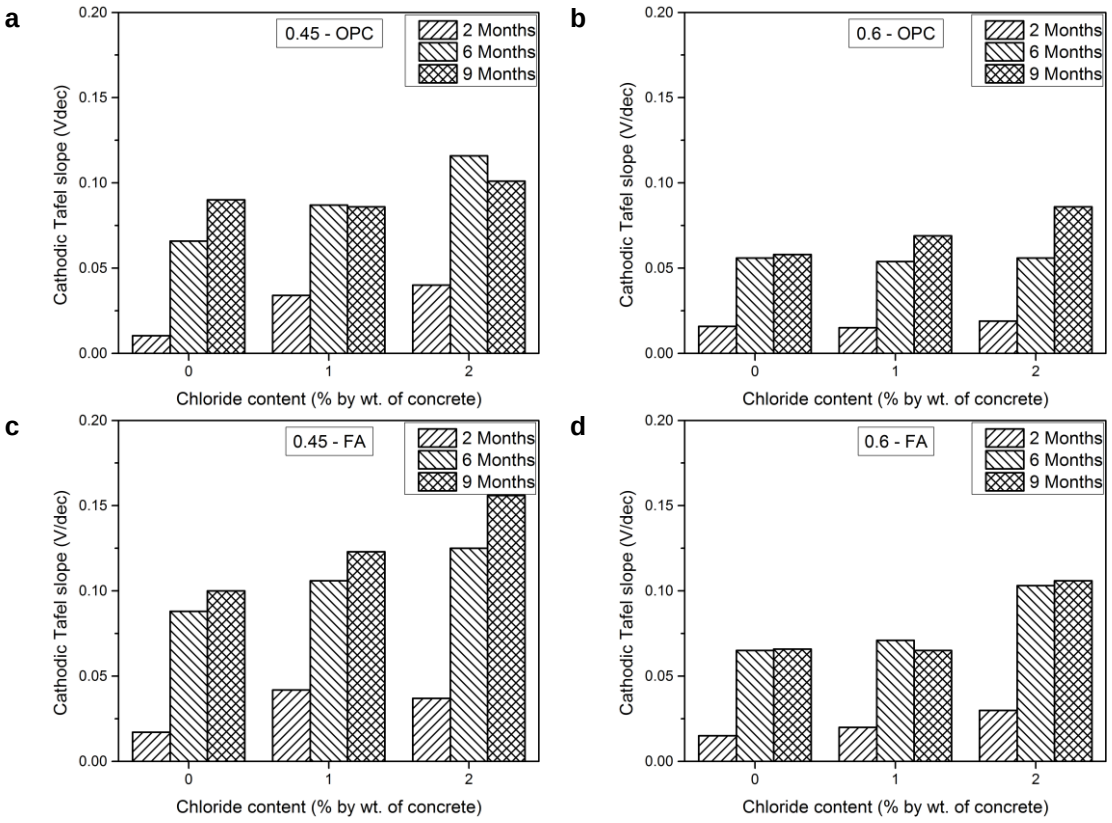

Fig. 7. Cathodic Tafel slope in (a-b) OPC concrete with W/B ratio (a) 0.45 and (b) 0.6 and (c-d) FA concrete with W/B ratio (c) 0.45 and (d) 0.6.

From experimental results, the magnitude of the cathodic Tafel slope was lower when the water to binder ratio increased due to high porosity. In contrast, the replacement of fly ash in concrete decreased the porosity of concrete. Hence, the cathodic Tafel slope of FA concrete was higher than that of OPC concrete. However, the effect of fly ash may take a long time and for that reason, the difference of the cathodic Tafel slopes of OPC and FA concrete was marginal at an early age.

For a longer time of exposure, the mentioned tendency was still observed. The effects of fly ash were more significant. In fact, concrete became denser with time. High humidity surrounding the specimen limited the oxygen ingress into the concrete. Consequently, the cathodic Tafel slope showed an upward tendency with time.

3.3. Equilibrium Potential – Φ^0

3.3.1. Anodic equilibrium potential

Experimental results of anodic equilibrium potential (Φ_a^0) are demonstrated in Fig. 8 for all series of specimens. Generally, at any period of exposure, the anodic equilibrium potential decreases with an increase in chloride content in concrete. After 2 months of exposure, the anodic equilibrium potential of chloride-free OPC concrete (0.45 W/B, -500 mV), is higher than that of chloride-contaminated concrete (-1000 mV). This influence of chloride ions on the anodic equilibrium potential was also found by Hussain and Ishida [13]. For a longer exposure period, the mentioned pattern of anodic

equilibrium potential can be observed. For example, after 9 months of exposure, the anodic equilibrium potential of chloride-contaminated concrete is still lower, compared to that of chloride-free concrete.

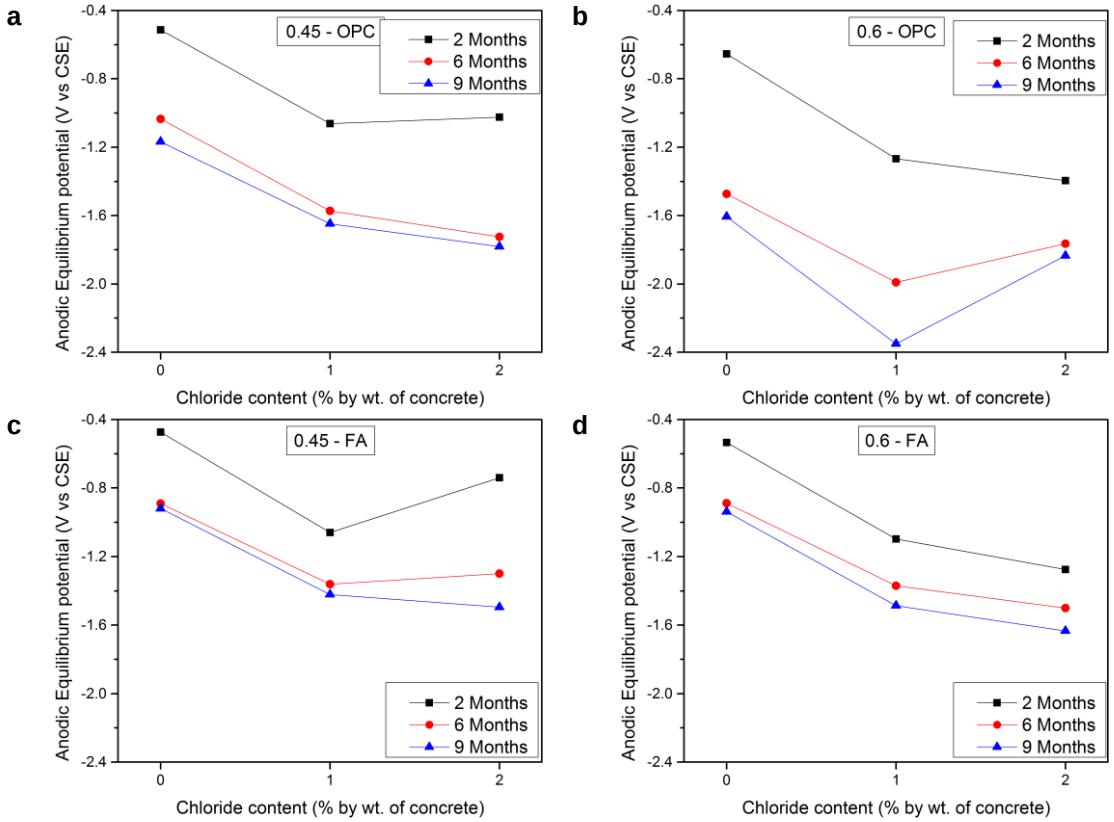

Fig. 8. Anodic equilibrium potential in (a-b) OPC concrete with W/B ratio (a) 0.45 and (b) 0.6 and (c-d) FA concrete with W/B ratio (c) 0.45 and (d) 0.6.

Besides the effects of chloride ions, the introduction of fly ash and a decrease in the water to binder ratio provided a similar tendency. Fly ash increased the anodic equilibrium potential of reinforcing steel. After 2 months of exposure, the anodic equilibrium potential in chloride-free OPC concrete (0.45 W/B, -500 mV) is lower than that of chloride-free FA concrete (-400 mV). Likewise, a lower water to binder ratio causes a higher (more positive) anodic equilibrium potential. In Fig. 8 (a-b), the anodic equilibrium potential of chloride-free OPC concrete (0.45 W/B, -500 mV) is higher than that of high W/B (0.6 W/B, -600 mV), after 2 months of exposure. A low water to binder ratio and fly ash provided a low porosity for concrete and restricted the movement of electrons between the anode and cathode on the steel surface. For these reasons, the anodic equilibrium potential tends to drift up.

Moreover, the anodic equilibrium potential decreased with time of exposure. The anodic equilibrium potential at 9 months of exposure was lower than that at 2 months of exposure while the corrosion current increases. The increase in corrosion current in a longer period was demonstrated in the section of the corrosion rate of reinforcing steel.

3.3.2. Cathodic equilibrium potential

Experimental results of the cathodic equilibrium potential (Φ_c^0) are summarized in Fig. 9 showing the influences of various factors. The cathodic equilibrium potential of reinforcing steel in chloride-free concrete was lower than that of chloride-contaminated concrete except for the case of a 2-month exposure, because the oxygen concentration in chloride-contaminated concrete is lower. As a result, the cathodic equilibrium potential is lower when the chloride content increases from 0% to 2%. This phenomenon could be observed after 6 months of exposure, which is caused by a low corrosion potential and a high corrosion current in this period of exposure. For a low corrosion potential (Fig. 4), or if the possibility of corrosion was high, an increase in corrosion current (Fig. 5) led to a higher cathodic equilibrium potential.

DOI:10.4186/ej.2020.24.3.23

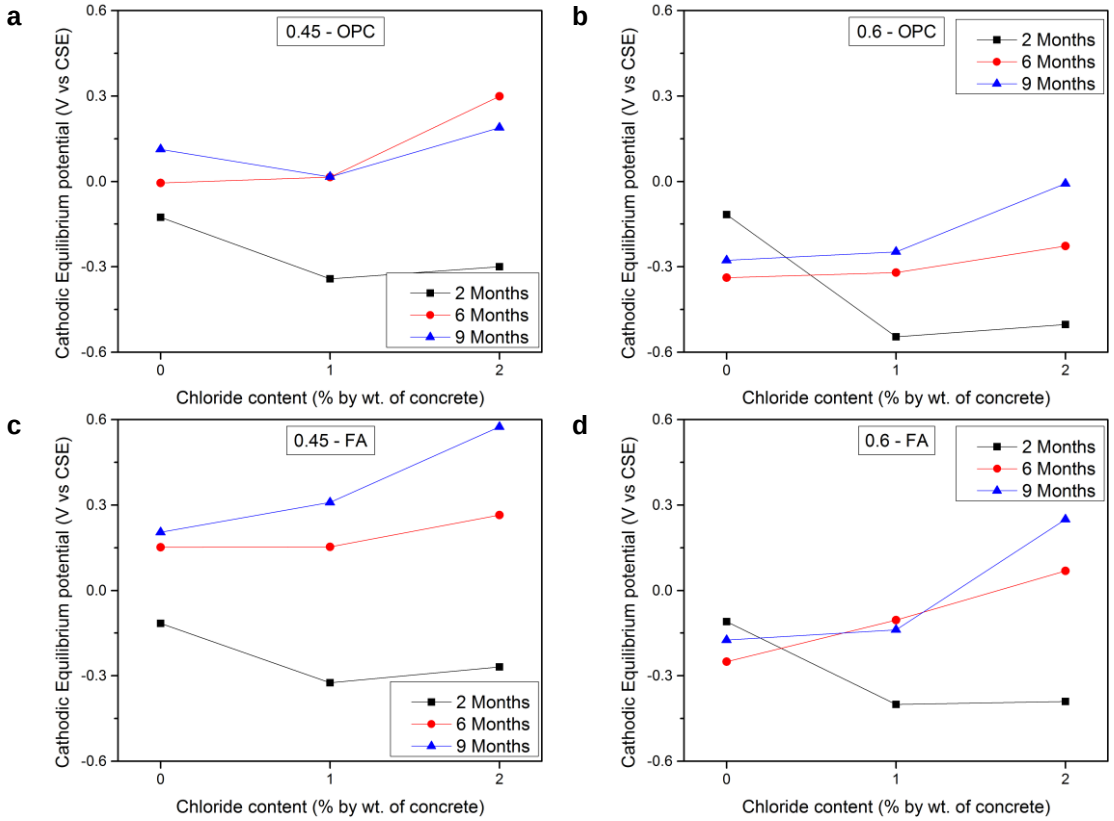

Fig. 9. Cathodic Equilibrium potential in (a-b) OPC concrete with W/B ratio (a) 0.45 and (b) 0.6 and (c-d) FA concrete with W/B ratio (c) 0.45 and (d) 0.6.

In contrast, at an early age, the corrosion potential of chloride-free concrete is significantly higher (less negative) than that in chloride-contaminated concrete, indicating a lower possibility of corrosion. This gap of potential is attributed to the existence of chloride ions in concrete, which accelerates the damage of passive films. Consequently, there is a drop of the cathodic equilibrium potential at 2 months from 0% to 1% [Cl^-]. At a longer period, this fall of cathodic equilibrium potential cannot be observed, because the corrosion potential of steel in chloride-free concrete was lower in accordance with time of exposure.

Decreasing the water to binder ratio increasing cathodic equilibrium potential. At 6 months of exposure, the cathodic equilibrium potential in chloride-free OPC concrete (0.45 W/B, 0 mV), is higher than that of high W/B concrete (0.6 W/B, -330 mV). At this point, the limitation of oxygen contributed to this increase in the cathodic equilibrium potential. The lower W/B concrete decreased the availability of oxygen in concrete, according to the result of the cathodic Tafel slope (Fig. 7). This causes a lower possibility of corrosion and a lower corrosion current in a low W/B concrete, as mentioned above. In Nernst equation (Eq. (3)), the influence of oxygen is described by the partial pressure, which is expected to be higher with a decrease in the W/B ratio. As a consequence, the cathodic equilibrium potential increases in low W/B concrete. Although low W/B concrete provides a higher pH, compared with high W/B concrete, this increase in pH could make the cathodic equilibrium potential higher, as expressed in Eq. (3), but this result is not observed here. This is because the variation in pH due to W/B ratio is not significant, to reverse the influence of limitation of oxygen.

Equations (2) and (3) [33] are Nernst equation for calculating equilibrium potential. As can be seen, the equilibrium potential depends on the activity of ferrous ions, pH, temperature, and pressure of oxygen.

$$\Phi_a^0 = -0.44 + \frac{2.303RT}{2F}\log\left(\left[Fe^{2+}\right]\right) \quad (2)$$

$$\Phi_c^0 = 0.40 + \frac{2.303RT}{2F}\log\left(\frac{p_{O_2}}{\left[OH^-\right]^4}\right) \quad (3)$$

The cathodic equilibrium potential in FA concrete was higher than that in OPC concrete. The cathodic polarization curve was shifted upwards with decreasing of pH which is caused by introducing fly ash into the concrete. Furthermore, the low porosity of FA concrete limits the availability of oxygen, based on the cathodic Tafel slope. For these reasons, the cathodic equilibrium potential in FA concrete was higher than that in OPC concrete.

In this study, the cathodic equilibrium potential increased considerably at a long time exposure. The same tendency can be seen in both chloride-free and chloride-contaminated concrete. This result is attributed to the

increase in corrosion current with time of exposure (Fig. 5). The unexpected increase in the cathodic equilibrium potential at 2 months (Fig. 9(b-d)) could be due to the high porosity of 0.6 W/B concrete, because this increase did not exist in 0.45 W/B concrete.

4. Conclusions

Based on the experimental results, the following conclusions were made:

(1) The experimental results showed that the electrochemical properties of reinforcing steel depended on various factors, including: chloride content, pH level, moisture content, electrical resistivity, etc. Individual parameter such as the Tafel slope cannot fully characterize the corrosion behavior of steel in concrete, but all of the parameters must be considered.

(2) The corrosion potential decreased while the corrosion rate increased with the presence of chloride ions in concrete. The corrosion potential was higher in low water to binder ratio and fly ash concrete.

(3) Fly ash decreased the pH of concrete, which was attributed to more polarized reinforcing steel in terms of anodic Tafel slope. However, fly ash reduced the amount of free chloride and the porosity of concrete. Therefore, the corrosion rate of reinforcing steel in fly ash concrete was lower, compared to that in OPC concrete.

(4) Based on electrochemical properties of reinforcing steel obtained in this study, the model of corrosion of steel in concrete would be developed in the future study.

It is worth mentioning that these electrochemical properties of steel, Tafel slope and equilibrium potential, are required in numerical studies of reinforcement corrosion. Since these properties are significant parameters to simulate the polarization behavior of steel during the corrosion process. From this perspective, a numerical model of corrosion could be conducted to predict corrosion behavior of reinforcing steel in the future study.

Acknowledgements

The authors would like to acknowledge the National Metal and Materials Technology Center for supporting the equipment during the research and the Center of Excellence in Material Science, Construction and Maintenance Technology Project, Thammasat University. This study was supported by Chair Professor Grant (P-19-52302), the National Science and Technology Development Agency (NSTDA), Thailand. The authors would like to thank Prof. Supapan Serapin for a fruitful discussion and proof reading.

References

[1] M. V. Tran and D. V. P. Tran, "Effect of thermal-humid media on durability of CFRP-wrapped reinforced concrete columns," presented at the CIGOS 2017, Ho Chi Minh City, Viet Nam, 2017.

[2] D. V. P. Tran, P. Sancharoen, P. Klomjit, and S. Tangtermsirikul, "Factors affecting half-cell potential profile of patching repaired concrete," in *The 3rd ACF Symposium 2019*, Sapporo, Japan, 2019.

[3] M. V. Tran and D. V. P. Tran, "Effect of temperature and humidity cycling on reinforcement corrosion," in *The 11th SEATUC Symposium*, Viet Nam, 2017.

[4] D. V. P. Tran, P. Sancharoen, P. Klomjit, and S. Tangtermsirikul, "Electrochemical compatibility of patching repaired reinforced concrete: experimental and numerical approach," *Journal of Adhesion Science and Technology,* pp. 1-21, 2019.

[5] M. V. Tran, D. V. P. Tran, and M. M. A. B. Abdullah, "Effect of Interrupting Electricity Period on Electrochemical Chloride Extraction of Reinforced Concrete," *Applied Mechanics and Materials,* vol. 754-755, pp. 342-347, 2015.

[6] S. W. Hnin, P. Sancharoen, and S. Tangtermsirikul, "Effects of concrete mix proportion on electrical resistivity of concrete," *Materials Science Forum,* vol. 866, pp. 68-72, 2016.

[7] S. W. Hnin, P. Sancharoen, and S. Tangtermsirikul, "Effects of mix proportion on electrical resistivity of concrete with fly ash," *ASEAN Engineering Journal,* vol. 7, pp. 53-65, 2017.

[8] D. Im, P. Sancharoen, P. Julnipitawong, and S. Tangtermsirikul, "Effects of chloride content on thermal properties of concrete," *International Journal of GEOMATE,* vol. 14, pp. 135-142, 2018.

[9] D. Im, P. Sancharoen, P. Julnipitawong, and S. Tangtermsirikul, "Effect of chloride and corrosion of reinforcing steel on thermal behavior of concrete and its modeling," *Engineering Journal,* vol. 22, pp. 143-163, 2018.

[10] M. Prazák, "The polarization resistance method for corrosion testing," *Material and Corrosion,* vol. 25, pp. 104-112, 1972.

[11] M. Stern, "A method for determining corrosion rates from linear polarization data," *Corrosion,* vol. 14, no. 9, pp. 60-64, 1958.

[12] K.-I. Kanno, M. Suzuki, and Y. Sato, "Tafel slope determination of corrosion reaction by the coulostatic method," *Corrosion Science,* vol. 20, pp. 1059-1066, 1980.

[13] R. R. Hussain and T. Ishida, "Enhanced electro-chemical corrosion model for reinforced concrete under severe coupled action of chloride and temperature," *Construction and Building Materials,* vol. 25, pp. 1305-1315, 2011.

[14] A. Bentur, S. Diamond, and N. Berke, *Steel Corrosion in Concrete: Fundamentals and Civil Engineering Practice*. London: E & FN Spon, 1997.

[15] *Standard Specification for Portland Cement*, ASTM C 150, 2007.
[16] *Standard Specification for Concrete Aggregates*, ASTM C 33, 2010.
[17] *Coal Fly Ash for Use as An Admixture in Concrete*, TIS 2135-2545, 2003.
[18] K. G. Robert, S. R. John, S. W. David, and B. G. Rudolph, *Electrochemical Techniques in Corrosion Science and Engineering*. New York, Basel: Marcel Dekker, Inc., 2003.
[19] X. L. Zhang, Z. H. Jiang, Z. P. Yao, Y. Song, and Z. D. Wu, "Effects of scan rate on the potentiodynamic polarization curve obtained to determine the Tafel slopes and corrosion current density," *Corrosion Science,* vol. 51, pp. 581-587, 2009.
[20] *Calculation of Corrosion Rates and Related Information from Electrochemical Measurements*, ASTM G 102, 1999.
[21] R. P. Roberge, *Corrosion Engineering Principles and Practice*. The McGraw-Hill Companies, 2008.
[22] *Standard Test Method for Corrosion Potentials of Uncoated Reinforcing Steel in Concrete*, ASTM C 876, 2015.
[23] L. Bertolini and E. Redaelli, "Throwing power of cathodic prevention applied by means of sacrificial anodes to partially submerged marine reinforced concrete piles: Results of numerical simulations," *Corrosion Science,* vol. 51, no. 9, pp. 2218-2230, 2009.
[24] J. P. Broomfield, *Corrosion of steel in concrete: Understanding, Investigation and Repair*. London, UK: E & FN Spon, 1997.
[25] K. Menzel and H. Preusber, "A non-destructive technique to detect corrosion of rebars," *Bauingenieur,* vol. 64, pp. 181-186, 1989.
[26] R. P. W. Vassie, "Evaluation of techniques for investigating the corrosion of steel in concrete," in *TRRL Supplementary Report 39*. London: Transport and Road Research Laboratory, 1978.
[27] K. Y. Ann and H.-W. Song, "Chloride threshold level for corrosion of steel in concrete," *Corrosion Science,* vol. 49, pp. 4113-4133, 2007.
[28] H.-W. Song, C.-H. Lee, and K. Y. Ann, "Factors influencing chloride transport in concrete structures exposed to marine environments," *Cement and Concrete Composites,* vol. 30, pp. 113-121, 2008.
[29] A. L. A. Fraay, J. M. Bijen, and Y. M. D. Haan, "The reaction of fly ash in concrete. a critical examination," *Cement and Concrete Research,* vol. 19, pp. 235-246, 1989.
[30] V. Saraswathy, S. Muralidharan, K. Thangavel, and S. Srinivasan, "Influence of activated fly ash on corrosion-resistance and strength of concrete," *Cement & Concrete Composites,* vol. 25, pp. 673-680, 2003.
[31] E. Schindelholz, B. E. Risteen, and R. G. Kelly, "Effect of relative humidity on corrosion of steel under sea salt aerosol proxies - I NaCl," *Journal of The Electrochemical Society,* vol. 161, no. 10, pp. 450-459, 2014.
[32] J. Ge and O. B. Isgor, "Effect of Tafel slope, exchange current density and electrode potential on the corrosion of steel in concrete," *Materials and Corrosion,* vol. 58, pp. 573-582, 2007.
[33] Y.-S. Ji, W. Zhao, M. Zhou, H.-r. Ma, and P. Zeng, "Corrosion current distribution of macrocell and microcell of steel bar in concrete exposed to chloride environments," *Construction and Building Materials,* vol. 47, pp. 104-110, 2013.

Dong Viet Phuong Tran, photograph and biography not available at the time of publication.

Pakawat Sancharoen, photograph and biography not available at the time of publication.

Pitichon Klomjit, photograph and biography not available at the time of publication.

Somnuk Tangtermsirikul, photograph and biography not available at the time of publication.